OncoTargets and Therapy

Dovepress
open access to scientific and medical research

Open Access Full Text Article

ORIGINAL RESEARCH

RETRACTED ARTICLE: LncRNA SNHG7 Functions as an Oncogene in Cervical Cancer by Sponging miR-485-5p to Modulate JUND Expression

This article was published in the following Dove Press journal:
OncoTargets and Therapy

Danyang Zhao[1,*]
Hui Zhang[2,*]
Jianxiong Long[3]
Mujun Li[1]

[1]Department of Reproductive Center, The First Affiliated Hospital of Guangxi Medical University, Nanning, Guangxi Province, People's Republic of China; [2]Department of Obstetrics, Chongzuo People's Hospital, Chongzuo, Guangxi Province, People's Republic of China; [3]School of Public Health of Guangxi Medical University, Nanning, Guangxi Province, People's Republic of China

*These authors contributed equally to this work

Background: Long non-coding RNA (LncRNA) SNHG7 is involved in the development of multiple cancers. However, its role in cervical cancer (CC) has not been elucidated. This study aimed to explore the function of SNHG7 in CC progression and the underlying mechanisms.
Materials and Methods: The expression levels of SNHG7 and miR-485-5p in CC tissues and cell lines were measured by qPCR. Functional experiments including CCK-8 assay, wound healing assay, transwell assay, flow cytometry, Western blot, luciferases reporter assay and immunoprecipitation (RIP) were performed to explore the SNHG7/miR-485-5p/JUND pathway. Additionally, in vivo study was carried out by establishing tumor xenograft models.
Results: We found that SNHG7 was markedly enhanced in CC tissues and cell lines, and associated with poor clinical characteristics. In vitro, knockdown of SNHG7 inhibited CC cell proliferation, migration and invasion, as well as aggravated cell apoptosis. As to mechanism investigation, rescue experiments revealed that miR-485-5p inhibitor could partially reverse the effects on CC cells induced by SNHG7 knockdown. SNHG7 upregulated JUND expression via miR-485-5p. Moreover, tumor xenograft models were established to confirm the findings in vivo.
Conclusion: SNHG7 promoted CC progression through miR-485-5p/JUND axis. The SNHG7/miR-485-5p/JUND pathway might provide a novel therapeutic target for CC treatment.

Keywords: lncRNA SNHG7, cervical cancer, CC, miR-485-5p, JUND, cell proliferation

Introduction

Cervical carcinoma (CC) is the second most common malignant tumor in females.[1] CC is mainly caused by human papillomavirus (HPV) infection. Upon HPV infection, E6 and E7 oncoproteins begin to express and regulate downstream gene expressions, thus contributing to continuous cell proliferation to malignant transformation.[2] There are about 500,000 women get CC and 260,000 die from it every year.[3] Although the treatment technology of CC has been greatly improved, the 5-year overall survival rate is still poor and metastatic CC is incurable.[4,5] Thus, it is urgent to improve new therapeutic approaches. Understanding the underlying molecular mechanisms of CC development will contribute to CC treatment.

Long non-coding RNAs (LncRNAs) are a subclass of non-coding RNAs with more than 200 nucleotides.[6] Although they were considered as noises with no biological functions, increasing evidences revealed that lncRNAs play key roles in many processes, such as chromatin modulating, RNA processing and protein

Correspondence: Jianxiong Long
School of Public Health of Guangxi Medical University, No. 22 Shuangyong Road, Nanning 530021, Guangxi Province, People's Republic of China
Tel +86-158 0771 4732
Email longjx12345@163.com

Mujun Li
Department of Reproductive Center, The First Affiliated Hospital of Guangxi Medical University, No. 6 Shuangyong Road, Nanning 530021, Guangxi Province, People's Republic of China
Tel +86-182 9010 8786
Email sciencecid@126.com

submit your manuscript | www.dovepress.com
DovePress
http://doi.org/10.2147/OTT.S237802

expression regulation.[7] As to cancers, more and more lncRNAs are reported to play as oncogenes or suppressors in multiple tumor progressions.[8] For example, GHET1 could drive prostate cancer progression by regulating KLF2 thereby activating HIF-1alpha/Notch-1 signaling pathway.[9] TTN-AS1 promoted colorectal cancer proliferation via sponging miR-376a-3p and upregulating KLF15.[10] Small nucleolar RNA host gene 7 (SNHG7), with a length of 2157 bp, is a newly discovered lncRNA which was reported to enhance the progression of a series of cancer types, including pancreatic cancer,[11] lung cancer,[12] bladder cancer,[13] colorectal cancer[14] and esophageal cancer.[15] However, whether SNHG7 also play roles in CC development has not been elucidated.

lncRNAs are likely to function via sponging miRNAs, thereby regulating downstream target genes expression. miR-485-5p was predicted as a target of SNHG7 by informatics tool. Moreover, miR-485-5p was identified as a tumor suppressor in a series of cancers, including cervical cancer.[16] In this study, we aimed to investigate the effects on CC progression and the possible mechanisms.

Table 1 Characteristics of Cervical Cancer Patients

Characteristics Total	N 45	SNHG7 Expression		P value
		High (n=30)	Low (n=15)	
Age				
≥50	33	25	8	0.512
<50	12	5	7	
Tumor Size				
≥4	26	18	8	0.012*
<4	19	7	12	
FIGO Stage				
III–IV	18	10	8	0.026*
I–II	27	8	19	
Lymph-Node Metastasis				
Yes	21	15	7	0.018*
No	24	15	15	
Histological Grade				
Well	26	12	14	0.518
Moderate/Poorly	19	12	7	

Note: *P < 0.05 represents statistical differences.

Materials and Methods

Human Tissues

A total of 45-paired CC tissues and normal tissues were obtained from the First Affiliated Hospital of Guangxi Medical University. Patients had not received systemic or local treatment prior to surgical resection. Table 1 shows the clinicopathologic characteristics. Tissue samples were immediately treated with liquid nitrogen and stored at −80°C. Informed consent was signed by every patient. Written informed consent was obtained from every involved patient. The Ethics Committee of the First Affiliated Hospital of Guangxi Medical University approved this study.

Cell Culture

CC cell lines (Hela, SiHA, C-33A and HT-3), human normal cervical cell line (Ect1/E6E7) and HEK-293T cells were purchased from Cell Bank of the Chinese Academy of Sciences (Shanghai, China) and incubated in DMEM (Gibco, USA) plus with 10% FBS and 1% penicillin-streptomycin (Beyotime, China). Cells were cultured in a humidified atmosphere with 5% CO_2 at 37°C.

RT-qPCR

Total RNA was extracted from tissues or cells using Trizol (Invitrogen, USA) following the protocol. The isolated RNA was then reverse-transcribed into cDNA with the help of MMLV (Promega, Wuhan). cDNA was taken as template and qPCR was conducted on a PikoReal Real-Time PCR System (ThermoFisher Scientific, USA) with SYBR GREEN SMART KIT (Tiangen, Nanjing, China). The expression levels of target genes were calculated by $2^{-\Delta\Delta Ct}$ method. U6 was used to normalize the relative expression level of miR-485-5p, while β-Actin was used for normalization of SNHG7 and JUND expressions. Specific primers are listed in Table 2.

CCK-8 Assay

CCK-8 assay was conducted to assess the viability of CC cells using CCK-8 Assay Kit (Dojindo, Toyoto). In brief, cells were seeded into 96-well plates with a concentration of 2×10^3 cells/well. After incubation of indicated hours, we added 100μL fresh medium and 10μL CCK-8 reagent into each well of 96-well plates (Corning, USA). Two hours later, optical density was measured at 450 nm daily using a microplate reader (ThermoFisher Scientific, USA).

Flow Cytometry

Cell apoptosis was detected using a FITC/PI Apoptosis Kit (Thermo, USA). Forty-eight hours after transfection, Annexin V binding buffer was taken to suspend cells.

Table 2 Primers of qRT-PCR

Gene	Primers	
SNHG7	Forward Reverse	5′- CGATACCATTGAACACGCTGC −3’ 5′- GGTTGAGGGTCCCAGTG −3’
miR-485-5p	Stem-loop RT primer Forward Reverse	5′- GTCGTATCCAGTGCAGGGTCCGAGGTATTCGCACTGGATACGACGAATTC −3’ 5′ AGAGGCTGGCCGTGATG-3’ 5′- GTGCAGGGTCCGAGGT −3’
JUND	Forward Reverse	5′-AGGACTTGCACAAGCAGAAC −3’ 5′-GTTGGCGTACACGGGCGGCT-3’
β-Actin	Forward Reverse	5′- AGCCACATCGCTCAGACAC −3’ 5′- GCCCAATACGACCAAATCC −3’
U6	Forward Reverse	5′- GCTTCGGCAGCACATATACTAAAAT −3’ 5′- CGCTTCACGAATTTGCGTGTCAT −3’

Then, Annexin V/FITC was added in the dark. Five minutes later, PI was added and apoptosis was analyzed by FACSAria I/II flow cytometer (BD Biosciences, USA).

Wound Healing Assay

Wound healing assay was applied to estimate cell migration rate. When transfected cells reached 90% confluence, a new micropipette tip was taken to make a scratch across the surface. PBS was used to wash the suspended cells and FBS-free DMEM (Gibco, USA) was added. Twenty-four hours later, images of cells were taken by a light microscope (Olympus, Japan).

Transwell Assay

Transwell assay was conducted to determine the cell invasion ability. The upper chamber of a transwell plate (Corning, USA) was coated with Matrigel (BD, USA). Complete medium with 10% FBS was added into the lower chamber. Twenty-four hours after transfection, the lower chamber was added with 70% ethanol and 0.1% crystal violet. The invaded cells were stained and counted from five visual fields which were randomly chosen.

Luciferase Reporter Assay

miR-NC or miR-485-5p mimics was co-transfected with SNHG7 mut or SNHG7 wt into HEK-293T cells for 48 h. Dual-luciferase reporter assay (Promega) was carried out according to the protocol. Similarly, miR-NC or miR-485-5p mimics was co-transfected with JUND mut or JUND wt, and dual-luciferase reporter assay (Promega, USA) was conducted subsequently.

Western Blot

Total protein was isolated from tissues or cells by RIPA (Sangon Shanghai, China). Equal amounts of each sample were loaded and separated by 10% SDS-PAGE. Proteins were transferred from gel to PVDF membranes (Millipore, USA) and blocked with 5% silk milk for 1 h. at room temperature. The membranes were then incubated with specific primary antibodies: anti-JUND (1:1000, CST, Beijing); anti-β-Actin (1:2500, CST, Beijing) overnight at 4°C. Subsequently, the membranes were incubated with HRP-conjugated antibody for 2 h at normal temperature. The blot signals were washed by TBST and visualized with an ECL Kit (Solarbio, Beijing, China). Images were taken by an ImageQuant LAS4000 Biomolecular Imager (GE Healthcare).

Immunohistochemical Staining

Ki67 expression was estimated via incubation in monoclonal antibody against Ki67 (1:500, CST, USA) at 4°C overnight. Subsequently, the samples were washed by PBS for three times and incubated with biotin-labeled IgG secondary antibody (1:500, SCT, USA). After 1 h, the samples were treated with HRP-conjugated streptavidin (CST, USA) and developed by DAB. Signals were visualized by EnVision system (Dako, Glostrup, Denmark).

Animal Experiments

Four-week-old BALB/C nude mice were purchased from Shanghai LAC Laboratory (Shanghai, China) and randomly divided into 2 groups (6 mice/group). Hela cells that were transfected with sh-NC or sh-SNHG7 stably were injected into flanks of mice. Then, the tumor volumes

were detected every week. After 5 weeks, mice were sacrificed and the weights of tumors were measured. Then, the tumor tissues were collected for following experiments to detect the expressions of miR-485-5p, JUND and Ki67. Ethical and legal approval was obtained from Ethics Committee of the First Affiliated Hospital of Guangxi Medical University prior to the commencement of the study. All experiments were performed following the guidelines and regulations of Ethics Committee of the First Affiliated Hospital of Guangxi Medical University.

Statistical Analysis

Data were presented as mean±standard deviation (SD). Each sample for experiments were repeated at least 3 times. SPSS 17.0 and Graphpad Prims6 was taken for statistical analysis. Student's *t*-test was applied for the difference between two groups and one-way ANOVA was for comparisons among multiple groups. P<0.05 suggested statistically significant.

Results

SNHG7 Was Upregulated in CC Tissues and Cell Lines

To explore the role of SNHG7 in CC development, the first step for us was to detect the expression pattern of SNHG7 in CC tissues and cell lines. As shown in Figure 1A, SNHG7 expressed markedly more in CC tissues than the normal tissues. Similarly, SNHG7 expressed a higher level in CC cell lines (Hela, SIHA, C-33A and HT-3) than in normal cervical cell line (Ect1/E6E7) (Figure 1B). Additionally, CC patients with higher SNHG7 expression levels have poorer overall survivals (Figure 1C).

SNHG7 Knockdown Inhibited CC Proliferation, Migration and Invasion

To investigate the effects of SNHG7 on CC development, we performed functional experiments using SNHG7 siRNA (si-SNHG7). Figures 2A and S1 showed that both the two siRNAs against SNHG7 exerted significant knockdown efficiency, and we chose si-SNHG7#1 for the following experiments. Next, we transfected si-SNHG7 or negative control (si-NC) into CC cell lines. CCK-8 assay suggested that si-SNHG7 inhibited CC cell viability (Figure 2B). Flow cytometry assay showed a significant promotion in CC cell apoptosis after SNHG7 silencing (Figure 2C). Suppression of SNHG7 also inhibited CC cell migration (Figure 2D) and invasion (Figure 2E). These primary results indicated that SNHG7 might act as an oncogenic role in CC progression.

SNHG7 Acted as a ceRNA for miR-485-5p

To explore the potential mechanisms underlying SNHG7-regulated CC, we investigated the relationship between SNHG7 and miR-485-5p. StarBase 3.0 predicted the interacting sites of SNHG7 and miR-485-5p (Figure 3A), which was confirmed by the following luciferase reporter assay (Figure 3B). As expected, miR-485-5p was upregulated upon SNHG7 knockdown, and SNHG7 was

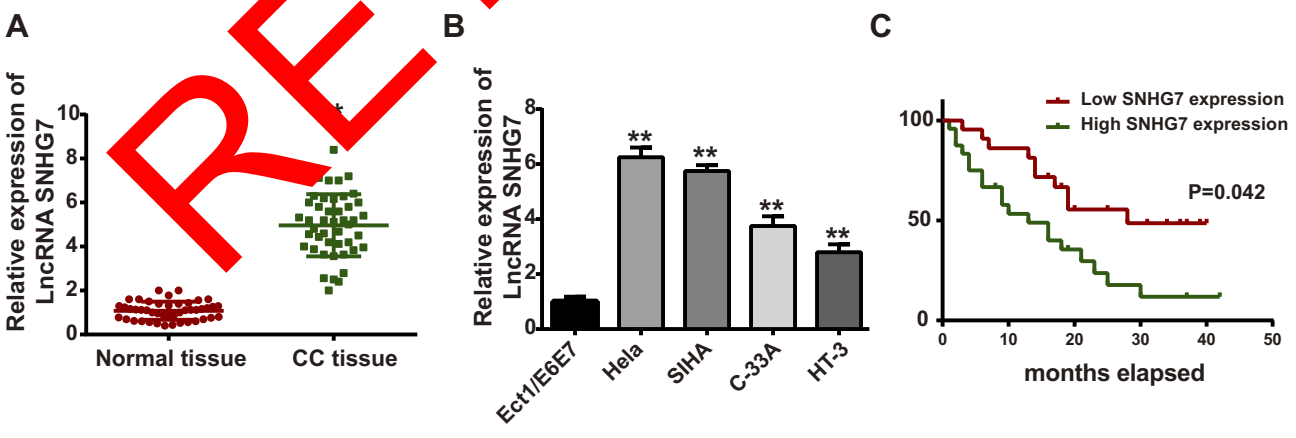

Figure 1 The upregulation of SNHG7 in CC tissues and cell lines. (**A**) Relative expression of SNHG7 in CC tissues and adjacent normal tissues was detected by qPCR. (**B**) Relative expression of SNHG7 in CC cell lines (Hela, SIHA, C-33A and HT-3) and normal cervical cells (Ect1/E6E7) was detected by qPCR. (**C**) The Kaplan–Meier curves of overall survivals with high and low SNHG7 expressions. **P<0.01.

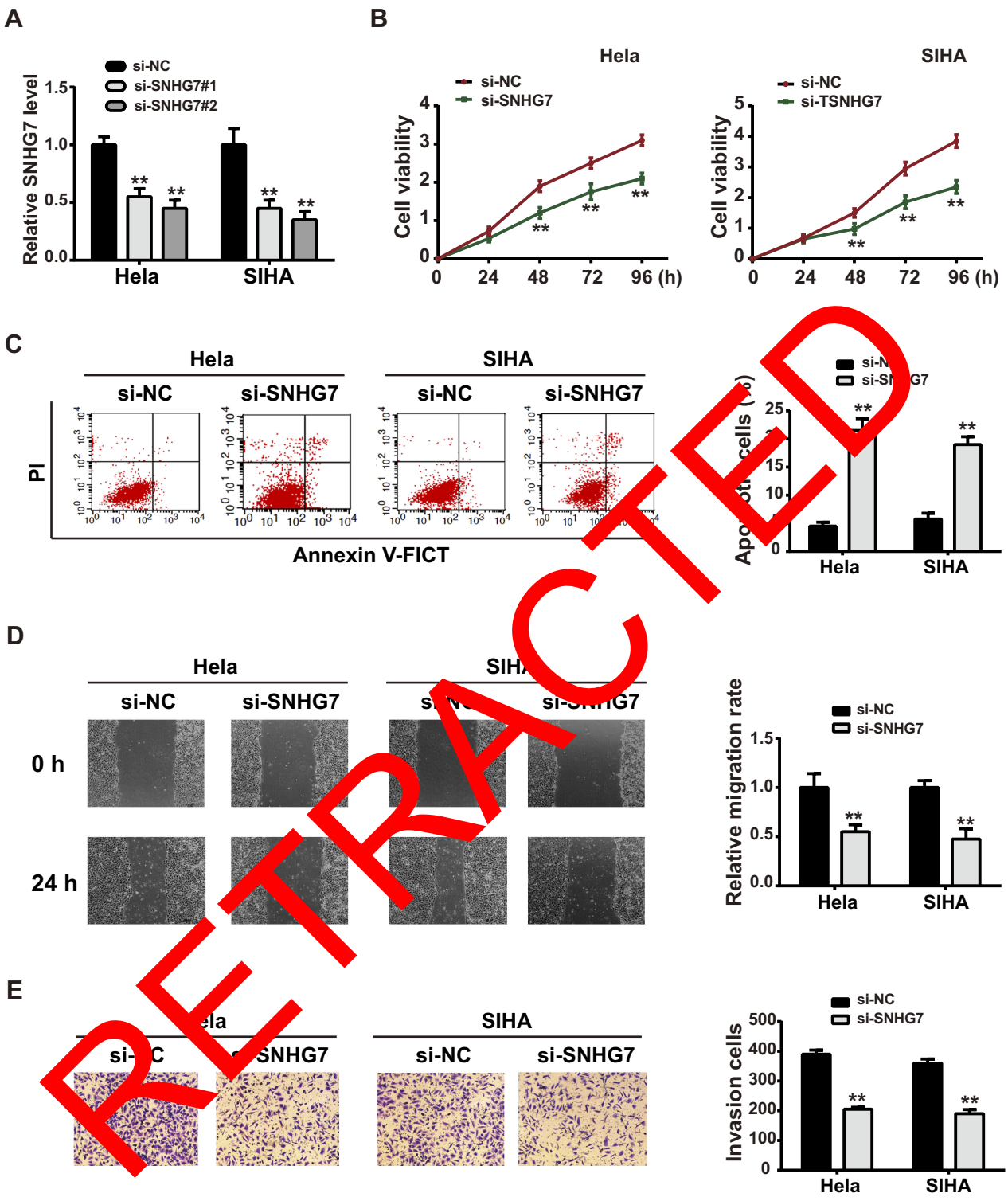

Figure 2 Knockdown of SNHG7 reduced CC cell proliferation, migration and invasion. (**A**) Relative expression of SNHG7 in EC cells was detected after SNHG7 siRNAs (si-SNHG7#1 and si-SNHG7#2) were transfected. (**B**) CCK-8 was conducted to estimate the cell viability. (**C**) Flow cytometry was performed to determine the cell apoptotic rate. (**D**) Wound healing assay was carried out to estimate the cell migration. (**E**) Transwell assay was conducted to measure the cell invasion ability. **P<0.01.

downregulated with miR-485-5p mimics transfection (Figure 3C and D). Moreover, RIP assay demonstrated that SNHG7 and miR-485-5p directly interacted in Ago2 complex (Figure 3E). Furtherly, SNHG7 was found downregulated in CC tissues (Figure 3F) and associated negatively with miR-485-5p expression (Figure 3G).

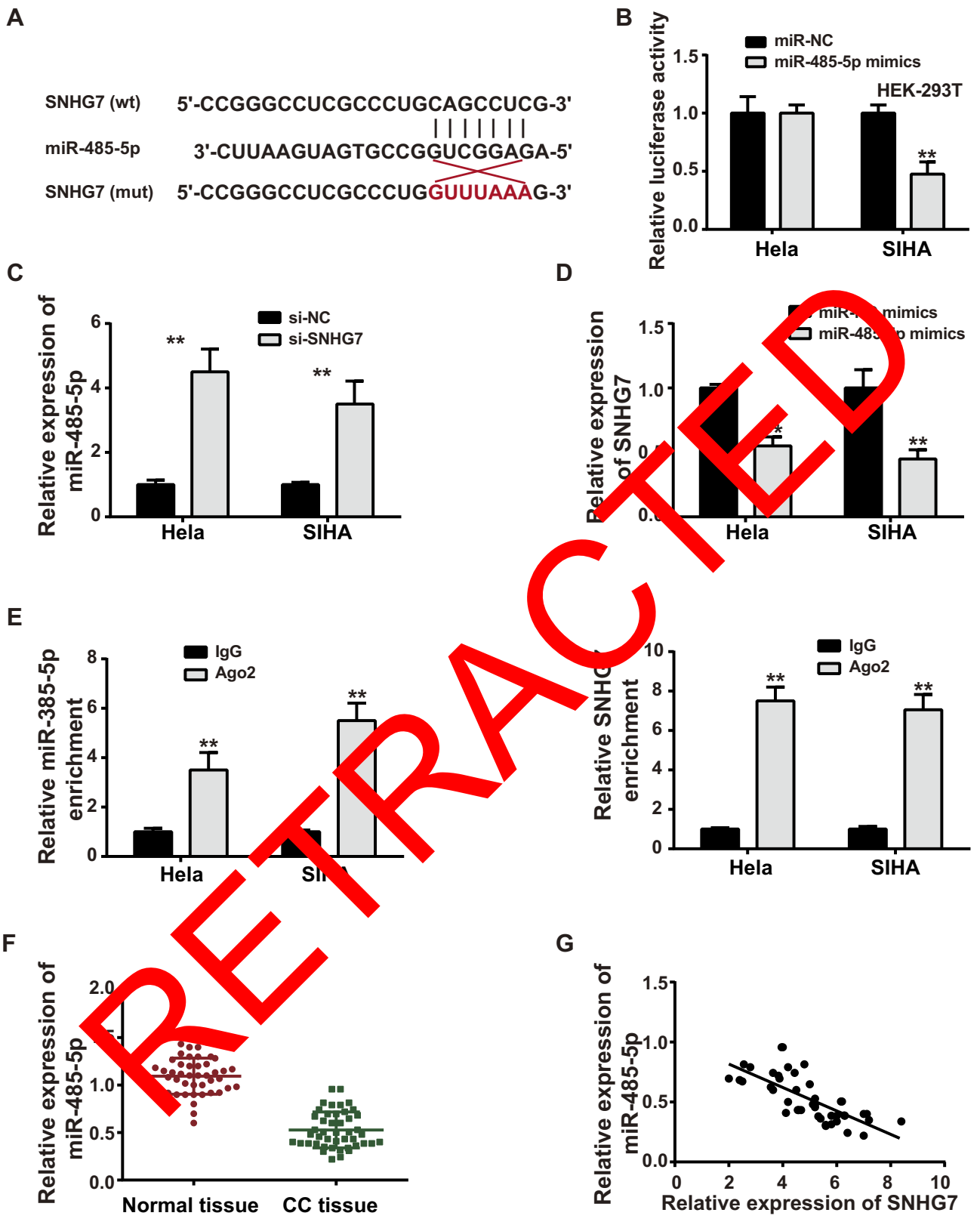

Figure 3 SNHG7 sponged miR-485-5p. (**A**) Predicted binding sites between SNHG7 and miR-485-5p from Starbase. (**B**) miR-NC mimics or miR-385a-5p mimics was co-transfected with SNHG7 mut or SNHG7 wt, and luciferase reporter assay was performed 48 h later. (**C**) si-NC or si-SNHG7 was transfected into EC cells, and the relative expression of miR-485-5p was detected by qPCR 48 h later. (**D**) miR-NC mimics or miR-485-5p mimics was transfected into EC cells, and the relative expression of miR-485-5p was detected by qPCR 48 h later. (**E**) The direct interaction between SNHG7 and miR-485-5p was detected by RIP with Ago-2 antibody. (**F**) The relative expression of miR-485-5p in CC tissues and adjacent normal tissues was measured by qPCR. (**G**) The relationship between SNHG7 and miR-485-5p in CC patients was analyzed by Pearson's correlation analysis. **P<0.01.

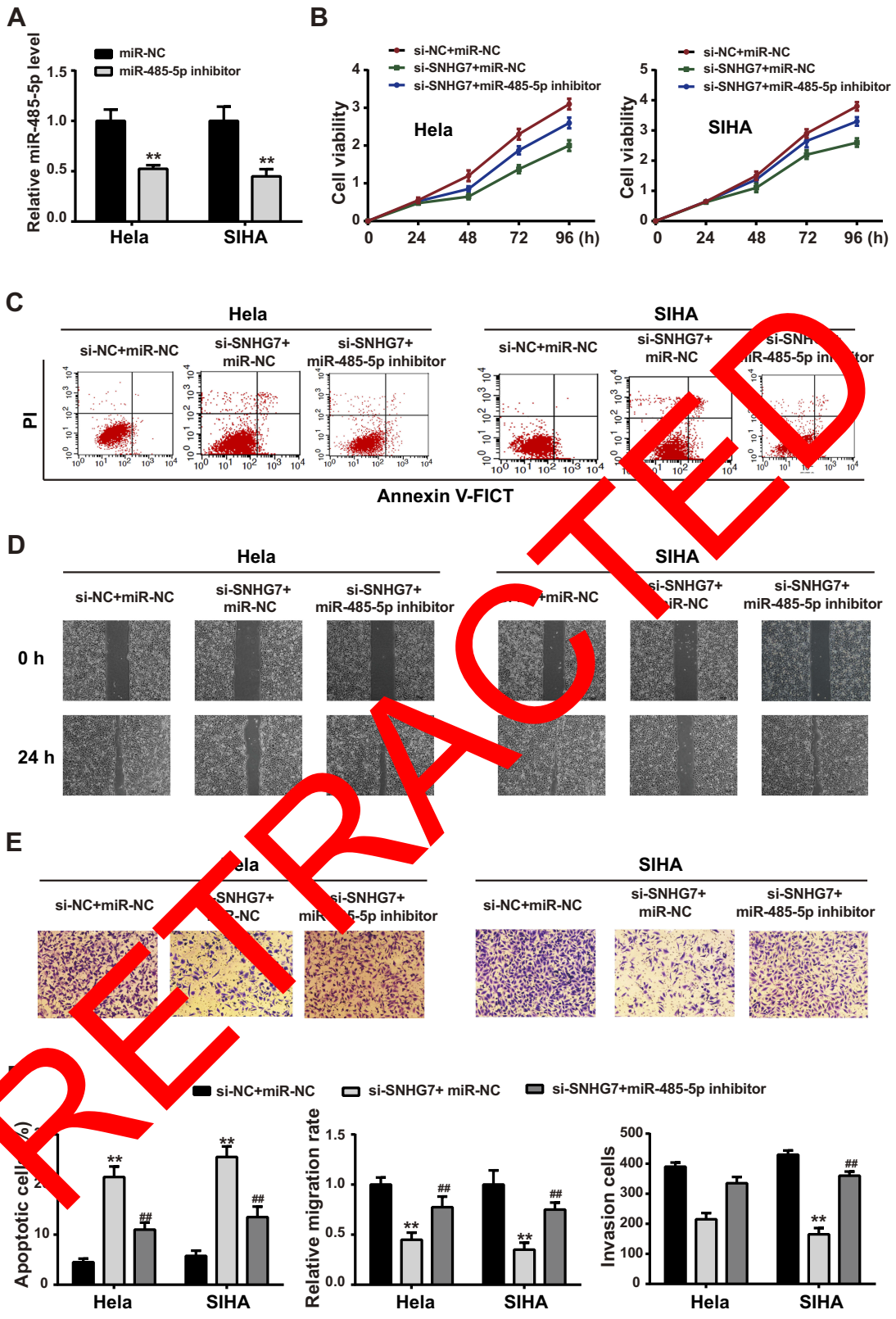

Figure 4 SNHG7-induced EC cell activity changes was mediated by miR-485-5p. (**A**) miR-485-5p expression was measured by qPCR with miR-485-5p inhibitor transfection. Then, EC cells were transfected with si-SNHG7 in the presence of miR-NC or miR-485-5p mimics, (**B**) cell viability was measured by CCK-8 assay; (**C**) cell apoptosis was determined by flow cytometry; (**D**) migration was detected by wound healing assay; (**E**) cell invasion was detected by transwell assay; (**F**) statistical assays were presented in bar graphs. **P<0.01 versus si-NC+miR-NC; ##P<0.01 versus si-SNHG7+miR-NC.

Suppression of miR-485-5p Partially Reversed the Effects of SNHG7 on CC Cells

To determine whether SNHG7 exhibited biological functions via miR-485-5p, we co-transfected miR-485-5p inhibitor or miR-NC with SNHG7 into CC cells. Figure 4A shows the inhibitory property of miR-485-5p inhibitor. Furtherly, miR-485-5p attenuated the suppression of SNHG7 on CC cell viability (Figure 4B), migration (Figure 4D) and invasion (Figure 4E). Also, depletion of miR-485-5p abolished the promotion of SNHG7 on CC cell apoptosis (Figure 4C). Figure 4F displays the quantitative analysis.

miR-485-5p Targeted JUND Directly

The bioinformatics TargetScan software revealed that miR-485-5p had complementary binding sites with JUND, which was verified by luciferase reporter assay (Figure 5A and B). JUND protein expression was inhibited

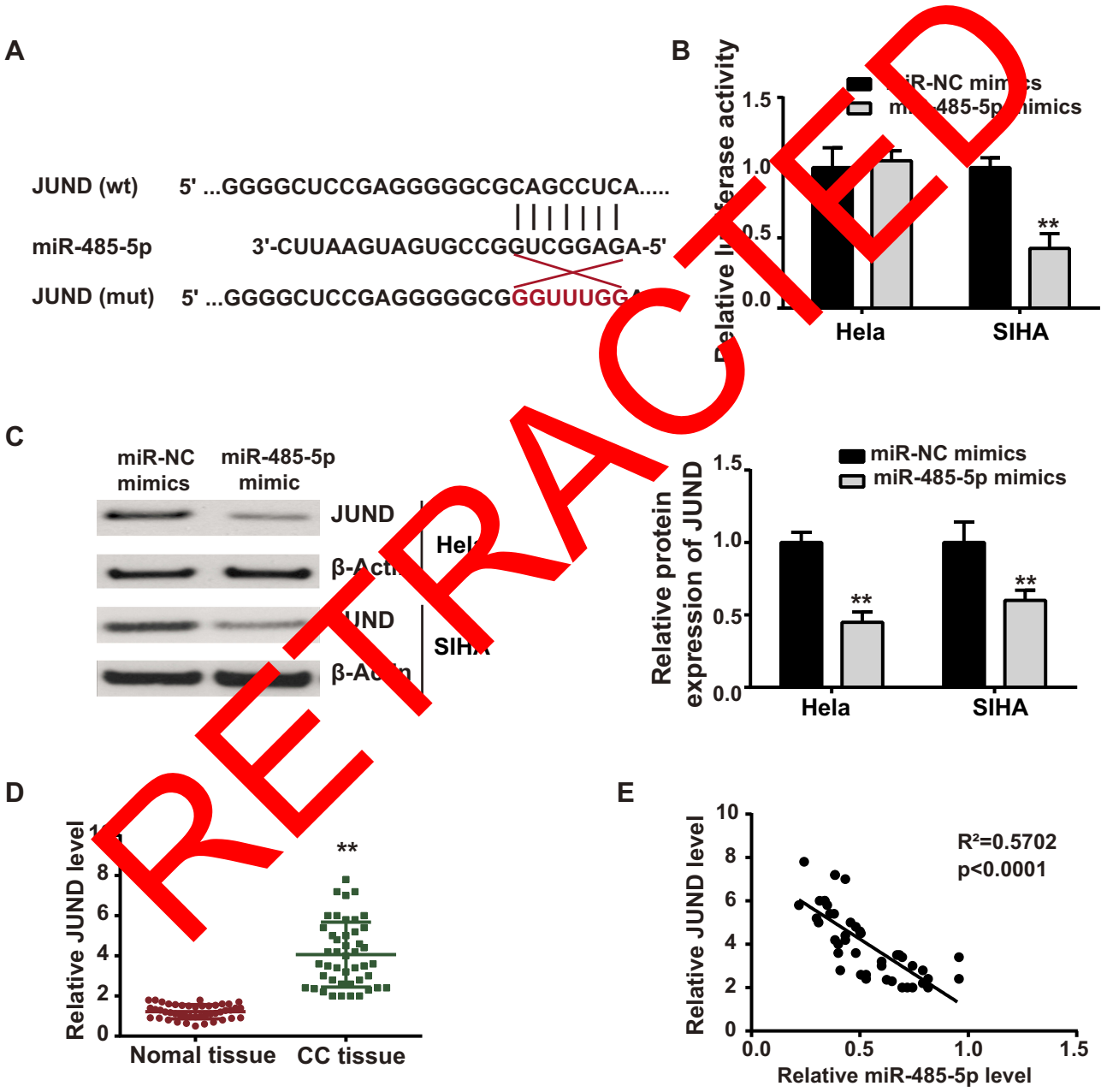

Figure 5 miR-485-5p directly targeted JUND. (**A**) Predicted binding sites between miR-485-5p and JUND from TargetScan. (**B**) miR-NC mimics or miR-485-5p mimics was co-transfected with JUND mut or JUND wt, and luciferase reporter assay was performed 48 h later. (**C**) miR-NC or miR-485-5p mimics was transfected into EC cells, and the relative expression of JUND was detected by Western blot 48 h later. (**D**) The relative expression of JUND in CC tissues and adjacent normal tissues was measured by qPCR. (**E**) The relationship between miR-485-5p and JUND in CC patients was analyzed by Pearson's correlation analysis. **P<0.01.

upon miR-485-5p overexpression (Figure 5C). Furtherly, we examined the expression profile of JUND in vivo and found that JUND expressed more in CC tissues than in normal tissues (Figure 5D). Additionally, JUND was negatively associated with miR-485-5p in CC tissues from patients (Figure 5E).

JUND Was Upregulated by SNHG7/miR-485-5p Axis

Previously found that SNHG7 sponged miR-485-5p (Figure 3) and miR-485-5p targeted JUND (Figure 5). Herein, we wanted to investigate whether SNHG7 could regulate JUND via miR-485-5p. As shown in Figure 6A–C, both mRNA and protein expression levels of JUND were downregulated upon SNHG7 depletion. However, miR-485-5p could mitigate the inhibitory effects. Moreover, SNHG7 and JUND showed positive relationship in CC tissues (Figure 6D).

SNHG7 Depletion Reduced Tumorigenesis in vivo

In vivo experiments were further conducted to validate the oncogenic function of SNHG7 in vitro. Xenograft tumor models were established in nude mice by injecting sh-NC or sh-SNHG7 stably transfected Hela cells. We observed that the tumor growth was more slowly in sh-SNHG7 implanted group than sh-NC group (Figure 7A). The tumor weight measured 5 weeks later was lighter in sh-SNHG7 mice, in

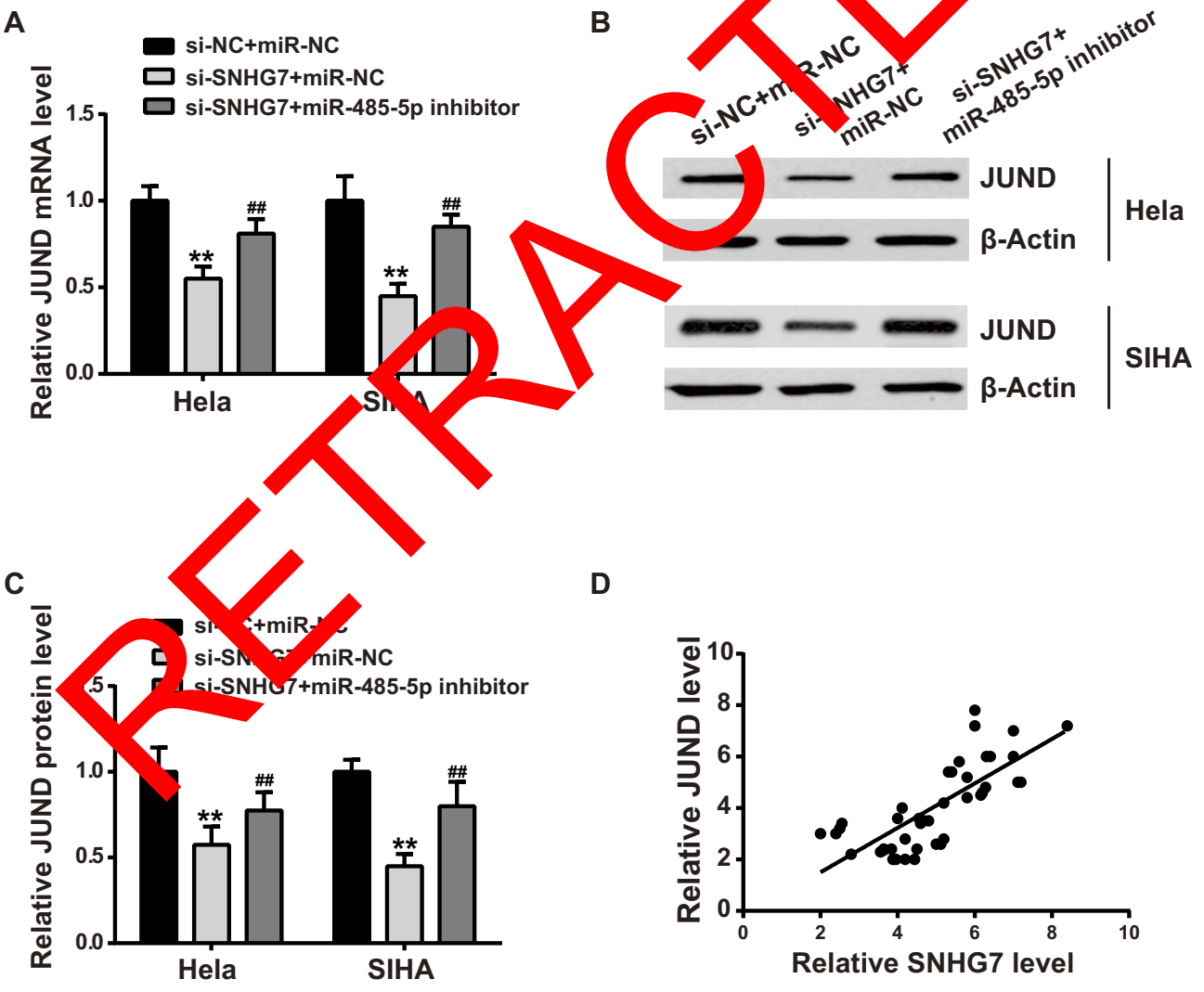

Figure 6 JUND was regulated by SNHG7/miR-485-5p axis. si-SNHG7 was co-transfected with si-NC or miR-485-5p inhibitor, then the mRNA and protein expression levels of JUND were estimated by qPCR (**A**) and Western blot (**B, C**). (**D**) The relationship between SNHG7 and JUND in CC patients was analyzed by Pearson's correlation analysis. **P<0.01 versus si-NC+miR-NC; ##P<0.01 versus si-SNHG7+miR-NC.

comparison with sh-NC group (Figure 7B). Moreover, the expression of miR-485-5p was elevated in sh-SNHG7 group (Figure 7C), whereas the JUND protein expression was lowly expressed (Figure 7D). IHC staining furtherly demonstrated that Ki67 was markedly upregulated by SNHG7 depletion (Figure 7E). These results indicated that SNHG7-regulated CC progression via sponging miR-485-5p and thereby upregulating JUND expression (Figure 8).

Discussion

Increasing study has reported that dysregulated lncRNAs were involved in the regulation of cancer progression.[17,18] A series of lncRNAs showed abnormal expressions in CC tissues, such as MNX1-AS1, HCP5, GAS5 and PVT1.[19–22] Also, SNHG7 was observed overexpressed in multiple cancer types and exhibited oncogenic roles in multiple cancer types. For example, SNHG7 enhanced cell viability, as well as inhibited cell apoptosis in gastric cancer.[23] Silencing of SNHG7 attenuating cell proliferation ability and driven cell apoptosis in thyroid cancer development.[24] SNHG7 knockdown inhibited EMT initiation and tumorigenesis in breast cancer.[25] However, whether SNHG7 influence CC progression has not been elucidated. Herein, our data revealed that SNHG7 was highly expressed in CC tissues, and depletion of SNHG7 reduced CC cell viability, migration and invasion, as well as enhanced apoptosis. The findings indicated that SNHG7 play oncogenic roles in CC development.

Acting as ceRNA for miRNAs was an important mechanism of lncRNA-regulating cancer progression. SNHG7 was reported to participate in cancer development by sponging miRNAs. For instance, SNHG7 sponged miR-381 to drive breast cancer.[26] Qi et al found SNHG7 acted as ceRNA for miR-503 to accelerate prostate cancer.[27] Han et al demonstrated that silencing of SNHG7 suppressed epithelial–mesenchymal transition in prostate cancer by targeting miR-324-3p.[28] Also, many lncRNAs were found to regulate CC by interacting with miRNAs. For example, STRG1 sponged miR-330-5p to enhance CC progression.[29] NEAT1 acted as an oncogene in CC by targeting miR-193a-3p.[30] In the present work, to explore the underlying mechanism of SNHG7-regulated CC development, we predicted miR-485-5p as the target of SNHG7. miR-485-5p exerted tumor-suppressive effects in multiple cancers, including hepatocellular carcinoma,[31] gastric cancer,[32] papillary thyroid cancer[33] and breast cancer.[34] Herein, we observed that miR-485-5p inhibitor

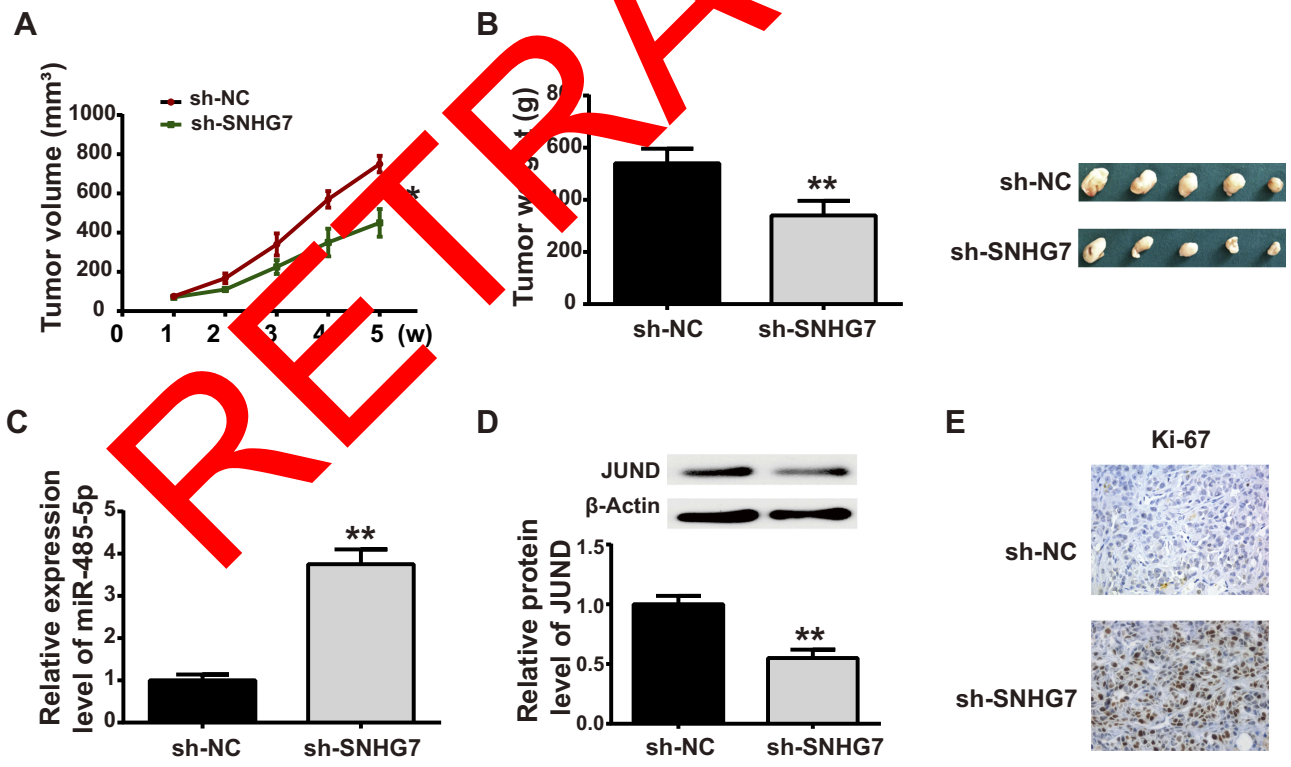

Figure 7 SNHG7 knockdown suppressed cervical tumor growth via miR-485-5p/JUND axis in vivo. Xenograft models were established by injecting sh-NC or sh-SNHG7 transfected HeLa cells into in the flanks nude mice, then (**A**) tumor volume was measured weekly; (**B**) tumor weight was measured 5 weeks later; (**C**) miR-485-5p mRNA expression was detected by qPCR; (**D**) JUND protein expression was detected by Western blot; (**E**) Ki67 was detected by IHC. **P<0.01 versus sh-NC. **P<0.01.

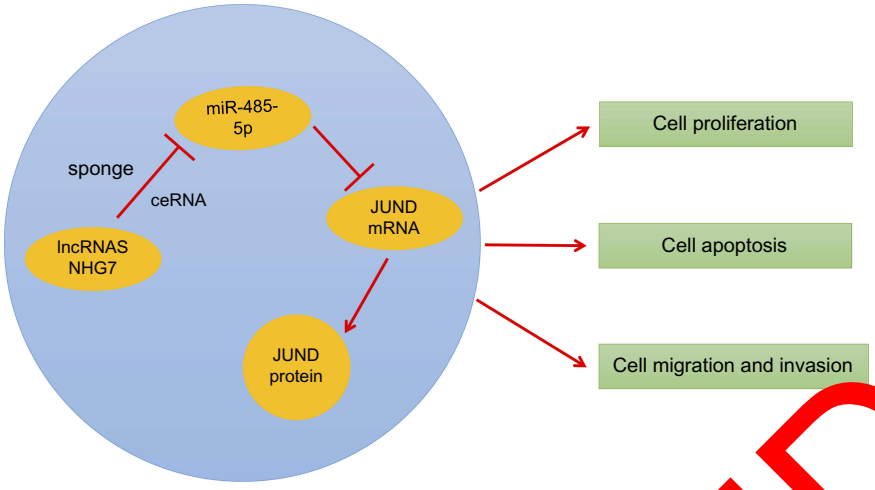

Figure 8 Diagram showing the regulation mechanism of SNHG7 in CC progression.

partially abolished the inhibitory effects of si-SNHG7 on CC cell viability, migration and invasion, indicating that SNHG7 promoted CC cell progression via miR-485-5p.

MiRNAs downregulate target mRNA expression through binding to 3′UTR seed region, which is the basis of lncRNA-miRNA-mRNA regulating network.[35] Yu et al revealed that HCP5 enhanced CC development through modulating miR-15a/MACC1 axis.[22] Gao et al demonstrated that SBF2-AS1 driven CC by regulating FOXM1 via miR-361-5p.[36] Ji et al showed that SNHG14 promoted CC development via acting as ceRNA for miR-206 to regulate YWHAZ.[37] In this work, we found jun D proto-oncogene (JUND) as the target gene of miR-485-5p using TargetScan software. JUND, a member of the AP-1 family, functioned as tumor-promoting role in some cancer types. For example, Elliott B reported that JUND was a crucial modulator in prostate cell cycle progression and thus promoting cancer development.[38] Ishikawa et al found that Butein ameliorated adult leukemia via inhibiting JUND expression. Cheng et al revealed that JUND was involved in cancer stemness and drug resistance in hepatocellular carcinoma.[40] Herein, luciferase assay confirmed the direct interaction between miR-485-5p and JUND. Moreover, SNHG7 positively regulated JUND via miR-485-5p, suggesting the SNHG7/miR-485-5p/JUND axis involved in the mechanism. Based on the characteristics that one lncRNA can sponge multi-miRNAs, and one miRNA also targets different genes, further study is needed to elucidate whether lncRNA-SNHG7 can regulate other miRNAs and proteins. This would help to understand the underlying mechanism of SNHG7-regulated cervical cancer progression better.

Conclusions

In conclusion, lncRNA SNHG7 played as an oncogene which promoted cell proliferation, migration and invasion by sponging miR-485-5p and thereby upregulating JUND (Figure 8). SNHG7.miR-485-5p/JUND axis might provide a novel approach for CC treatment.

Ethical Approval

Written informed consent was obtained from every involved patient. The Ethics Committee of the First Affiliated Hospital of Guangxi Medical University approved this study. All experiments were performed following the guidelines and regulations of Ethics Committee of the First Affiliated Hospital of Guangxi Medical University.

Funding

This work was supported by Youth Fund Project of Guangxi Natural Science Foundation (2017GXNSFBA198070) and Youth Fund Project of National Natural Science Foundation of China (81703290); Chongzuo Science and Technology Tackling (17111307); Chongzuo Science and Technology Bureau FA (2017021).

Disclosure

The authors declare that they have no competing interests in this work.

References

1. Boom K, Lopez M, Daheri M, et al. Perspectives on cervical cancer screening and prevention: challenges faced by providers and patients along the Texas-Mexico border. *Perspect Public Health*. 2019;139(4):199–205. doi:10.1177/1757913918793443

2. Almeida AM, Queiroz JA, Sousa F, et al. Cervical cancer and HPV infection: ongoing therapeutic research to counteract the action of E6 and E7 oncoproteins. *Drug Discov Today*. 2019;24(10):2044–2057. doi:10.1016/j.drudis.2019.07.011
3. Ferlay J, Soerjomataram I, Dikshit R, et al. Cancer incidence and mortality worldwide: sources, methods and major patterns in GLOBOCAN 2012. *Int J Cancer*. 2015;136(5):E359–E386. doi:10.1002/ijc.29210
4. Uyar D, Rader J. Genomics of cervical cancer and the role of human papillomavirus pathobiology. *Clin Chem*. 2014;60(1):144–146. doi:10.1373/clinchem.2013.212985
5. Kim JJ, Campos NG, Sy S, et al. Inefficiencies and high-value improvements in US cervical cancer screening practice a cost-effectiveness analysis. *Ann Intern Med*. 2015;163(8):589–+. doi:10.7326/M15-0420
6. Qi P, Du X. The long non-coding RNAs, a new cancer diagnostic and therapeutic gold mine. *Mod Pathol*. 2013;26(2):155–165. doi:10.1038/modpathol.2012.160
7. Geisler S, Coller J. RNA in unexpected places: long non-coding RNA functions in diverse cellular contexts. *Nat Rev Mol Cell Biol*. 2013;14(11):699–712. doi:10.1038/nrm3679
8. Yang GD, Lu XZ, Yuan LJ. LncRNA: a link between RNA and cancer. *Biochim Biophys Acta Gene Regul Mech*. 2014;1839(11):1097–1109. doi:10.1016/j.bbagrm.2014.08.012
9. Zhu YF, Tong Y, Wu J, et al. Knockdown of LncRNA GHET1 suppresses prostate cancer cell proliferation by inhibiting HIF-1 alpha/Notch-1 signaling pathway via KLF2. *Biofactors*. 2019;45(3):364–373. doi:10.1002/biof.v45.3
10. Wang Y, Jiang F, Xiong Y, Cheng X, Qiu Z, Song R. LncRNA TTN-AS1 sponges miR-376a-3p to promote colorectal cancer progression via upregulating KLF15. *Life Sci*. 2019;116936.
11. Cheng DF, Fan J, Ma Y, et al. LncRNA SNHG7 promotes pancreatic cancer proliferation through ID4 by sponging miR-342-3p. *Biosci*. 2019;9. doi:10.1186/s13578-019-0290-2
12. Chen K, Abuduwufuer A, Zhang H, et al. SNHG7 mediates cisplatin-resistance in non-small cell lung cancer by activating PI3K/AKT pathway. *Eur Rev Med Pharmacol Sci*. 2019;23(16):6936–6943. doi:10.26355/eurrev_201908_18733
13. Chen S, Li W, Guo A. LOXL1-AS1 predicts poor prognosis and promotes cell proliferation, migration, and invasion in leiomyosarcoma. *Biosci Rep*. 2019;39(4).
14. Li Y, Zeng C, Hu J, et al. Long noncoding RNA-SNHG7 acts as a target of miR-34a to increase GALNT7 level and regulate PI3K/Akt/mTOR pathway in colorectal cancer progression. *J Hematol Oncol*. 2018;11(1):89. doi:10.1186/s13045-018-0632-2
15. Long B, Li N, Xu X-X, et al. Long noncoding RNA LOXL1-AS1 regulates prostate cancer cell proliferation and cell cycle progression through miR-541-3p and CCND1. *Biochem Biophys Res Commun*. 2018;505(2):561–568. doi:10.1016/j.bbrc.2018.09.160
16. Ou R, Lv X, Zhang L, et al. CircMOTL1 motivates AMOTL1 expression to facilitate cervical cancer growth. *Mol Ther Nucleic Acids*. 2020;18:459–470. doi:10.1016/j.omtn.2019.09.022
17. Caceres-Gutierrez R, Herrera LA. Centromeric Non-coding transcription: opening the black box of chromosomal instability? *Curr Genomics*. 2017;18(3):227–235. doi:10.2174/1389202917666161102095508
18. Gutschner T, Diederichs S. The hallmarks of cancer: a long non-coding RNA point of view. *RNA Biol*. 2012;9(6):703–719. doi:10.4161/rna.20481
19. You Z, Liu C, Wang C, et al. LncRNA CCAT1 promotes prostate cancer cell proliferation by interacting with DDX5 and MIR-28-5P. *Mol Cancer Ther*. 2019;18(12):2469–2479. doi:10.1158/1535-7163.MCT-19-0095
20. Ma -T-T, Zhou L-Q, Xia J-H, et al. LncRNA PCAT-1 regulates the proliferation, metastasis and invasion of cervical cancer cells. *Eur Rev Med Pharmacol Sci*. 2018;22(7):1907–1913. doi:10.26355/eurrev_201804_14713
21. Yang W, Hong L, Xu X, et al. LncRNA GAS5 suppresses the tumorigenesis of cervical cancer by downregulating miR-196a and miR-205. *Tumour Biol*. 2017;39(7):1010428317711315. doi:10.1177/1010428317711315
22. Yu Y, Shen H-M, Fang D-M, et al. LncRNA HCP5 promotes the development of cervical cancer by regulating MACC1 via suppression of microRNA-15a. *Eur Rev Med Pharmacol Sci*. 2018;22(15):4812–4819. doi:10.26355/eurrev_201808_15616
23. Wang M-W, Liu J, Liu Q, et al. LncRNA SNHG7 promotes the proliferation and inhibits apoptosis of gastric cancer cells by repressing the P15 and P16 expression. *Eur Rev Med Pharmacol Sci*. 2017;21(20):4613–4622.
24. Wang Y-H, Huo B-L, Li C, et al. Knockdown of long noncoding RNA SNHG7 inhibits the proliferation and promotes apoptosis of thyroid cancer cells by downregulating [illegible]. *Eur Rev Med Pharmacol Sci*. 2019;23(11):4815–4827. doi:10.26355/eurrev_201906_18067
25. Sun X, Huang T, Liu Z, et al. LncRNA SNHG7 contributes to tumorigenesis and progression of breast cancer by interacting with miR-34a through EMT induction and the Notch-1 pathway. *Eur J Pharmacol*. 2019;856:172407. doi:10.1016/j.ejphar.2019.172407
26. Gao Y-T, Zhou Y-C, Long non-coding RNA (lncRNA) small nucleolar RNA host gene 7 (SNHG7) promotes breast cancer progression by sponging miR-381. *Eur Rev Med Pharmacol Sci*. 2019;23(15):6588–6595. doi:10.26355/eurrev_201908_18545
27. Qi H, Wen B, Wu Q, et al. Long noncoding RNA SNHG7 accelerates prostate cancer proliferation and cycle progression through cyclin D1 by sponging miR-503. *Biomed Pharmacother*. 2018;102:326–332. doi:10.1016/j.biopha.2018.03.011
28. Han Y, Hu H, Zhu J. Knockdown of LncRNA SNHG7 inhibited epithelial-mesenchymal transition in prostate cancer though miR-324-5p/WNT5A axis in vitro. *Pathol Res Pract*. 2019;215(10):152537. doi:10.1016/j.prp.2019.152537
29. Zhang Y, Hu G-M, Wang W-L, et al. LncRNA TDRG1 functions as an oncogene in cervical cancer through sponging miR-330-5p to modulate ELK1 expression. *Eur Rev Med Pharmacol Sci*. 2019;23(17):7295–7306. doi:10.26355/eurrev_201909_18834
30. Han D, Wang J, Cheng G. LncRNA NEAT1 enhances the radioresistance of cervical cancer via miR-193b-3p/CCND1 axis. *Oncotarget*. 2018;9(2):2395–2409. doi:10.18632/oncotarget.v9i2
31. Peng Y, Leng W, Duan S, et al. Long noncoding RNA BLACAT1 is overexpressed in hepatocellular carcinoma and its downregulation suppressed cancer cell development through endogenously competing against hsa-miR-485-5p. *Biomed Pharmacother*. 2019;116:109027. doi:10.1016/j.biopha.2019.109027
32. Kang M, Ren M-P, Zhao L, et al. miR-485-5p acts as a negative regulator in gastric cancer progression by targeting flotillin-1. *Am J Transl Res*. 2015;7(11):2212–2222.
33. Zhang Y, Hu J, Zhou W, Gao H. LncRNA FOXD2-AS1 accelerates the papillary thyroid cancer progression through regulating the miR-485-5p/KLK7 axis. *J Cell Biochem*. 2018 Nov 19.
34. Lou C, Xiao M, Cheng S, et al. MiR-485-3p and miR-485-5p suppress breast cancer cell metastasis by inhibiting PGC-1alpha expression. *Cell Death Dis*. 2016;7:e2159. doi:10.1038/cddis.2016.27
35. Huang Y, Shen XJ, Zou Q, et al. Biological functions of microRNAs. *Bioorg Khim*. 2010;36(6):747–752. doi:10.1134/s1068162010060026
36. Gao FY, Feng J, Yao H, Li Y, Xi J, Yang J. LncRNA SBF2-AS1 promotes the progression of cervical cancer by regulating miR-361-5p/FOXM1 axis. *Artif Cells Nanomed Biotechnol*. 2019;47(1):776–782. doi:10.1080/21691401.2019.1577883
37. Ji NN, Wang Y, Bao G, Yan J, Ji S. LncRNA SNHG14 promotes the progression of cervical cancer by regulating miR-206/YWHAZ. *Pathol Res Pract*. 2019;215(4):668–675. doi:10.1016/j.prp.2018.12.026

38. Elliott B, Millena AC, Matyunina L, et al. Essential role of JunD in cell proliferation is mediated via MYC signaling in prostate cancer cells. *Cancer Lett*. 2019;448:155–167. doi:10.1016/j.canlet.2019.02.005
39. Ishikawa C, Senba M, Mori N. Butein inhibits NF-kappaB, AP-1 and Akt activation in adult T-cell leukemia/lymphoma. *Int J Oncol*. 2017;51(2):633–643. doi:10.3892/ijo.2017.4026
40. Cheng BY, Lau EY, Leung H-W, et al. IRAK1 augments cancer stemness and drug resistance via the AP-1/AKR1B10 signaling cascade in hepatocellular carcinoma. *Cancer Res*. 2018;78(9):2332–2342. doi:10.1158/0008-5472.CAN-17-2445